JOURNAL OF CATALYSIS 138, 746–749 (1992)

NOTES

XAFS Study of Molybdenum Oxide Catalysts on Various Supports

In a previous paper (*1*), the present authors reported that the hydrogenation (HYD) and hydrocracking (HYC) activities of molybdenum sulfide catalysts are significantly affected by the support. The order of the supports for HYC catalytic activity was $TiO_2 \gg SiO_2 > Al_2O_3 > MgO$ and for HYD activity $Al_2O_3 > TiO_2 > MgO > SiO_2$. As a result of the characterization of these catalysts, we found that the catalytic activities of the sulfide catalysts depended strongly on the structures of the starting calcined oxide catalyst. In the present study, X-ray absorption fine structure (XAFS) analyses (extended X-ray absorption fine structure (EXAFS) and X-ray absorption near-edge structure (XANES)) have been used to obtain a better understanding of the support effects on the structure of the calcined catalysts. In particular, the focus of the discussion is on the coordination symmetry around Mo, since the XAFS technique gives direct information on the local structure around specific atoms.

Commercially available γ-Al_2O_3 (170 m^2/g), SiO_2 (266 m^2/g), MgO (51 m^2/g), and laboratory-prepared TiO_2 (66 m^2/g) were used as catalyst supports. Two series of catalysts containing 2 or 10 wt% molybdenum as MoO_3 were prepared by wet impregnation, followed by drying and calcining at 500°C. Details of the preparation procedures are described in a previous paper (*1*). Each sample analyzed by EXAFS was powdered and pressed at ambient conditions into a pellet with a proper thickness for transmission measurement. The Mo *K*-absorption EXAFS spectra of the catalysts were measured at the Photon Factory (beam line BL-10B) in the National Laboratory for High Energy Physics. Fourier transformation of the $k/f(k)$-weighted EXAFS data was performed to obtain the radial distribution function around molybdenum. The phase shift and back-scattering amplitude ($f(k)$) were corrected by using the theoretical values for molybdenum as an absorber and oxygen as a scatterer (*2*).

Figure 1 shows the Fourier transforms of the EXAFS spectra for the catalysts. All the spectra have a peak due to Mo–O scattering at 1.8 Å. However, the peak position is slightly different in each spectrum and the peak height is highly dependent on the support. These features of the Mo–O peak reflect the local structure around Mo.

To determine the contributions from tetrahedral (Tet) and octahedral (Oct) structures, the first coordination shell (0.64 Å $< r <$ 2.01 Å) was simulated in *k*-space (2.5 $Å^{-1} < k <$ 17 $Å^{-1}$). The Debey–Waller factor (σ^2), the kinetic energy of the outgoing electrons (ΔE_0), and the shake-up factor (S_0) of each shell used in the simulation were obtained by fitting the EXAFS data of $Na_2MoO_4 \cdot 7H_2O$ (Tet) and MoO_3 (Oct) to their respective crystallographic data (*4*). The parameter in the simulation was the fraction of tetrahedrally coordinated oxygen around Mo, $N_{Tet}/(N_{Tet} + N_{Oct})$, where N_{Tet} and N_{Oct} were the average numbers of oxygen with tetrahedral and octahedral coordination, respectively, around Mo. The total coordination number was kept constant using the relation $N_{Oct}/6 + N_{Tet}/4 = 1$.

The simulation results for the EXAFS data of the catalysts are shown in Table 1. Molybdate on the MgO support has predominantly a Tet structure irrespective of the metal loading between 2 and 10 wt%. On the other hand, the Tet structure is much less abundant than the Oct structure for cata-

0021-9517/92 $5.00

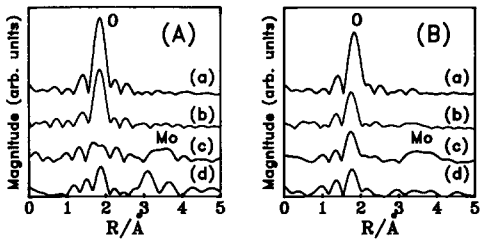

FIG. 1. Fourier transform EXAFS of molybdenum oxide catalysts supported on various oxides. (A) 2 wt% MoO_3: (a) MgO, (b) Al_2O_3, (c) SiO_2, (d) TiO_2. (B) 10 wt% MoO_3: (a) MgO, (b) Al_2O_3, (c) SiO_2, (d) TiO_2.

lysts supported on SiO_2 and TiO_2. For the Al_2O_3-supported catalyst, the fraction of the Tet structure decreases from 68 to 38% with increasing MoO_3 loading.

The Mo *K*-edge XANES data also give information on the coordination symmetry. The intensity of the pre-edge peak at 20.008 keV, which is assigned to the 1*s*–4*d* transition (*5*), can be used qualitatively as an index of the Tet structure (*6*). The XANES measurement of the present samples showed that the intensity of the pre-edge peak decreased in the order of MgO > Al_2O_3 > TiO_2 ≈ SiO_2 for the 2 wt% molybdate catalysts, while the 10 wt% catalysts showed the order MgO ≫ Al_2O_3 ≈ TiO_2 ≈ SiO_2. Thus, the XANES results are in good agreement with the EXAFS results shown in Table 1.

The specific surface area of the MgO support (66 m^2/g) is not high enough to disperse 10 wt% molybdate as isolated tetrahedra. This suggests that Tet MoO_4^{2-} anion is incorporated inside the MgO matrix. It is possible that bulk $MgMoO_4$ is formed during calcination by the reaction between wet MgO and molybdate as indicated by Oganowski (*7*).

The predominant structure of molybdate on the Al_2O_3 support changes from Tet to Oct with increasing Mo loading, although the total amount of the Tet structure does not decrease. This trend agrees with the result derived from laser Raman spectroscopy (LRS) studies (*8–10*), but disagrees with the result from a previous EXAFS study in which the average coordination number of oxygen around Mo decreased with increasing Mo loading (*11*). The high calcination temperature (550°C) employed in the EXAFS study might have caused the discrepancy with other studies including ours reported here.

Another EXAFS study (*6*) and a LRS study (*8*) indicated that isolated MoO_4^{2-} (Tet) was formed only on the basic OH groups on the surface of Al_2O_3. Two-dimensional polymolybdate with Oct symmetry is formed on other sites of the Al_2O_3 surface (*8–10*). Formation of bulk $Al_2(MoO_4)_3$ (Tet) was also suggested to take place to some extent during calcination depending on the calcination temperature (*9, 10*). Thus, the Al_2O_3 surface favors the formation of an Oct polymolybdate structure when the metal loading goes above a critical concentration and the catalyst is calcined at moderate temperatures.

The spectra of the SiO_2-supported catalysts (Fig. 1) have a peak at 3.5 Å, which is assigned to the nearest Mo–Mo scattering based on comparison with the spectrum of MoO_3. This result is consistent with the result from LRS (*1*), which showed the formation of a MoO_3-like structure on the SiO_2 support. On the other hand, no Mo–Mo peak was observed on the TiO_2 or Al_2O_3 supports. A previous EXAFS study by Kisfaludi *et al.* (*12*) showed that calcination of a physical mixture of MoO_3 and γ-Al_2O_3 dramatically decreased the Mo–Mo peak as a result of loss of long-range order in the MoO_3 particles. Thus, the absence of the Mo–Mo peak indicates that the Oct molyb-

TABLE 1

Simulation of EXAFS Data

Mo loading	2 wt%	10 wt%
MgO	0.87	0.73
Al_2O_3	0.68	0.38
SiO_2	0.20	0.17
TiO_2	0.28	0.13

date structures are highly disordered. It is possible that the two-dimensional polymolybdate structure suggested by LRS studies (*8–10*) does not give the Mo–Mo scattering peak because of extensive structural disorder.

A notable difference in the form of the molybdate is observed between the TiO_2- and Al_2O_3-supported catalysts. In contrast to the Al_2O_3 support, an Oct structure is predominantly formed on the TiO_2 support even when the molybdate loading was only 2 wt%. If the surface properties of TiO_2 are similar to those of Al_2O_3, isolated MoO_4^{2-} (Tet) should be observed on the TiO_2 support, even with the lower surface area of the TiO_2 (66 m^2/g) compared with that of the Al_2O_3 (170 m^2/g). The present result indicates that molybdate on TiO_2 does not favor Tet species on the surface nor in the bulk, but forms Oct polymolybdate.

The structure of molybdate supported on TiO_2 was analyzed by Ng and Gulari (*13*) who used LRS and IR spectroscopy. Their results indicated that a higher dispersion of polymolybdate was achieved on TiO_2 compared with Al_2O_3 when the catalysts were prepared by dry impregnation. A high dispersion of a monolayer of molybdate on TiO_2 was also suggested by ESR and XPS (*14*). Our present results reveal the cause for the above differences that occur with changing Mo loading for TiO_2 and Al_2O_3. Oct polymolybdate is homogeneously dispersed on TiO_2, while polymolybdate aggregates around Tet Mo species anchored to the Al_2O_3 surface.

In the second nearest shell region of the Fourier transform of the EXAFS data, the 2 wt% molybdate catalyst on TiO_2 showed a broad peak at 3.1 Å (Fig. 1). This peak might be due to Mo–Ti scattering (Mo–O–Ti). No significant peaks were observed around 3 Å for the other catalysts; however, the low back-scattering amplitude of Mg or Al would preclude Mo–Al or Mo–Mg scattering. Thus, it is not meaningful to discuss the homogeneity of the Mo–O–X bonding (X = Ti, Al, Si) based on the scattering of Mo–X in the EXAFS spectra when different support species are used.

Our results are consistent in many respects with the results suggested by LRS studies. That is, (a) the Tet molybdate structure is predominantly formed on MgO, (b) a MoO_3-like structure is formed on SiO_2, and (c) a polymolybdate structure with Oct coordination is formed on TiO_2 and Al_2O_3. In addition, our results indicated that Oct polymolybdate was formed on the TiO_2 support even at low Mo loadings. This result is in contrast to the LRS study by Ng and Gulari (*13*), in which they concluded that a significant amount of Tet molybdate coexists with Oct polymolybdate on TiO_2. However, it should be noted that the determination of Tet or Oct coordination on the base of a single Mo–O vibrational band is not straightforward, as has been pointed out by Schrader and Cheng (*15*).

ACKNOWLEDGMENT

The X-ray absorption measurements were carried out with the approval of the Photon Factory Program Advisory Committee (Proposal 85-006, 87-024).

REFERENCES

1. Shimada, H., Sato, T., Yoshimura, Y., Hiraishi, J., and Nishijima, A., *J. Catal.* **110,** 275 (1988).
2. Teo, B. K., and Lee, P. A., *J. Am. Chem. Soc.* **101,** 2815 (1979).
3. Matsumoto, K., Kobayashi, A., and Sasaki, Y., *Bull. Chem. Soc. Jpn.* **48,** 1009 (1975).
4. Kihlborg. L., *Ark. Kem.* **21,** 357 (1963).
5. Cramer, S. P., Hodgson, K. O., Gillum, W. O., and Mortenson, L. E., *J. Am. Chem. Soc.* **100,** 3398 (1978).
6. Mensch, C. T. J., van Veen, J. A. R., van Wingerden, B., and van Dijk, M. P., *J. Phys. Chem.* **92,** 4961 (1988).
7. Oganowski, J., Hanuza, J., Jezowska-Trzebiatowska, B., and Wrzyszcz, J., *J. Catal.* **39,** 161 (1975).
8. Jezirowski, H., and Knozinger, H., *J. Phys. Chem.* **83,** 1166 (1979).
9. Zingg, D. S., Mokovsky, L. E., Tischer, R. E., Brown, F. R., and Hercules, D. M., *J. Phys. Chem.* **84,** 2898 (1980).
10. Medema, J., van Stam, C., de Beer, V. H. J., Konings, A. J. A., and Koningsberger, D. C., *J. Catal.* **53,** 386 (1978).

11. Chiu, N.-S., Bauer, S. H., and Johnson, M. F. L., *J. Catal.* **89,** 226 (1984).
12. Kisfaludi, G., Leyrer J., Knözinger, H., and Prins, R., *J. Catal.* **130,** 192 (1991).
13. Ng, K. Y. S., and Gulari, E., *J. Catal.* **92,** 340 (1985).
14. Cáceres, C. V., Fierro, J. L. G., Lazaro, J., Agudo, A. L., and Soria, J., *J. Catal.* **122,** 113 (1990).
15. Schrader, G. L., and Cheng, C. P., *J. Phys. Chem.* **87,** 3675 (1983).

H. SHIMADA
N. MATSUBAYASHI
T. SATO
Y. YOSHIMURA
A. NISHIJIMA

National Chemical Laboratory for Industry
Tsukuba, Ibaraki, 305
Japan

N. KOSUGI[1]
H. KURODA[2]

Department of Chemistry
Faculty of Science
University of Tokyo
Hongo, Bunkyo-ku, 113 Tokyo
Japan

Received October 10, 1991; revised April 22, 1992

[1] Present address: Division of Engineering, Kyoto University, Yoshidahonmachi, Sakyo-ku, Kyoto, 606, Japan.

[2] Present address: Faculty of Science and Engineering, Science University of Tokyo, 2641, Yamasaki, Noda, Chiba, 278, Japan.